J. Info. Storage Proc. Syst., Vol. 3, 27–41, 2001

ISSN 1099-8047

Journal of Information Storage and Processing Systems

Optimal Track-Following Design for the Highest Tracks per Inch in Hard Disk Drives

Zhongming Li,[1,2] Guoxiao Guo,[2] Ben M. Chen,[1] and T.H. Lee[1]

[1]Department of Electrical Engineering, National University of Singapore, 119260, Singapore; [2]Data Storage Institute, DSI Building, No. 5, Engineering Drive 1, 117608, Singapore

Original manuscript received 30 June 2000; revised manuscript accepted 13 November 2000.

Abstract. *This paper presents an optimal track-following control design procedure that can find the theoretical highest tracks per inch (TPI) achievable in hard disk drives. By formulation of the hard disk drive servo system into an H_2 optimal control problem, achieving the highest achievable TPI is equivalent to minimizing the corresponding H_2 norm from the disturbances and noise to the true PES. Thus, the standard output feedback H_2 optimization procedure can be used. The design method is applied to a single-stage actuator system and a dual-stage actuator system, and the corresponding output feedback controllers have been found. Compared with other design approaches, a higher TPI rate can be achieved by the proposed method. The resultant TPI rate can be a criterion of evaluation of any other linear design work toward TPI budget improvement.*

Keywords. Hard disk drive; track misregistration (TMR); H_2 norm; H_2 optimal control.

1. Introduction

In recent years, the areal density of magnetic hard disk drives has been growing at 100% every year. The recording bit aspect ratio is expected to decrease from 20:1 to 4:1 and even further for the rotating magnetic recording systems of 100 Gbits/in.^{2} and above, as a result of the advantage of a better signal-to-noise ratio when the track density increases faster than the linear density. This rapid trend requires a significant improvement of the actuator positioning servo system. The $3\sigma_{\text{PES}\ t}$, that is, the standard deviation of the true position error signal or true PES (denoted as PES t), is often used as a measure of the tracking accuracy during the reading and writing operation. For a given mechanical system, improving the performance of the track-following controller to achieve a higher tracking accuracy is one of the cost-effective ways to increase the rate of tracks per inch (TPI).

Many control methods have been used to minimize the $3\sigma_{\text{PES}}$, which determines read–write tracking misregistration (TMR). These include LQG/LTR (Chang et al., 1997), optimal control (Iwashiro et al., 1999; Yamaguchi et al., 1999; Lin et al., 2000), robust control (Goh et al., 1999), multirate control (Chen et al., 1999; Fujimoto et al., 1999; Hara and Tomizuka, 1999), dual-stage actuator control (Aggarwal et al., 1997; Evans et al., 1999; Hernandez et al., 1999; Horsley et al., 1999; Semba et al., 1999), and so on. However, the highest achievable rate of TPI has not yet been fully investigated. If the highest achievable rate of TPI can be found, the control design effort toward a higher TPI by any other linear method can be evaluated.

This paper presents an optimal track-following control design approach that could minimize the $3\sigma_{\text{PES}\ t}$, of the hard disk drive servo system for given disturbance and noise models. This paper is arranged as follows. In Section 2 the relationship between the TMR and H_2 norm is established. After the corresponding H_2 output feedback problem of the hard disk drive (HDD) servo system is formulated, the algorithm is given. Section 4 presents the simulation results, using the proposed design method. Both the single-stage actuator servo system and the dual-stage actuator servo system are examined here. Finally, the concluding remarks are drawn in Section 5.

2. TMR and the H_2 Optimal Control Problem

In this section, the relationship between the TMR and the H_2 optimal control problem is first established. Then a

---

Presented at the 11th Annual Symposium on Information Storage and Processing Systems, Santa Clara, California, USA, 21–23 June 2000
Correspondence to: Zhongming Li

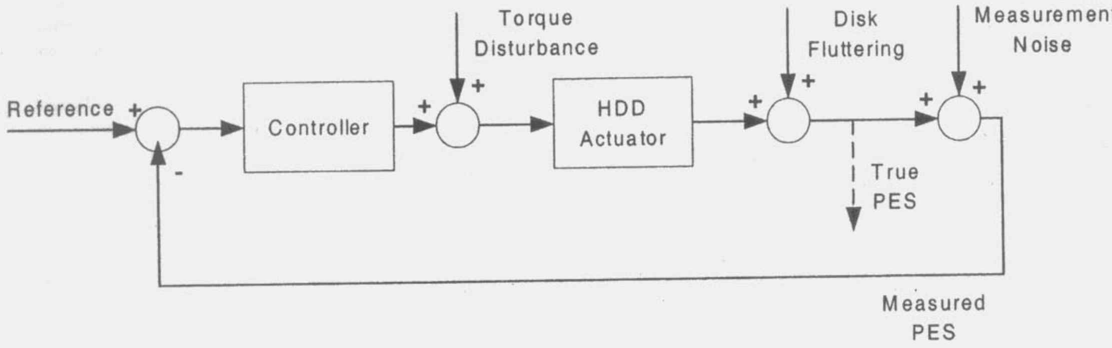

Fig. 1. Typical HDD servo system.

general description of an H_2 optimal output feedback control problem is given, followed by the algorithm to obtain the optimal controller. This algorithm allows us to design an optimal or suboptimal output feedback controller that can achieve the highest TPI rate in the HDD servo systems.

The structure of the typical HDD servo system is shown in Fig. 1. The actuator can be either a single-stage one or a dual-stage one. For simplicity of analysis, we assume that the repeatable runouts (RROs) are eliminated by some effective methods, such as feed-forward methods, without affecting the closed-loop stability. In this case, the nonrepeatable runout (NRRO), which can be classified into three categories; that is, input disturbance, output disturbance and measurement noise, is the key component that decides the read–write TMR (Abramovitch et al., 1997; Guo, 1997; Ho, 1997; Ehrlich and Curran, 1999; Yamaguchi et al., 1999).

The input disturbance refers to all the disturbances that act as torque disturbance, such as disturbances caused by the digital-to-analog (D/A) quantization noise, power driver noise, and the air-turbulence upon the actuator. The output disturbance refers to all the disturbances that are caused by nonrepeatable motions of the disk, which are directly added to the relative position of the read–write head and the servo track. Other noise sources such as media noise, servo demodulator noise, and the like can be considered as measurement noise (Ho, 1997; Hurst et al., 1997; McAllister, 1997; Ehrlich and Curran, 1999).

In order to achieve the highest TPI rate, one would have to minimize TMR subject to all the NRRO sources described above. For simplicity, we only considered $\sigma_{\mathrm{PES}\,t}$ as the source of TMR, where $\sigma_{\mathrm{PES}\,t}$ in Eq. (1) is the standard deviation of the true PES signal, $y_{\mathrm{PES}\,t}$ (Chang et al., 1997),

$$\sigma_{\mathrm{PES}\,t} = \sqrt{\frac{1}{n-1}\sum_{i=1}^{n} y_{\mathrm{PES}\,t}(i)^2} \tag{1}$$

Here n in Eq. (1) is the number of the true PES samples.

To associate $\sigma_{\mathrm{PES}\,t}$ with a control design problem, consider the H_2 norm and H_2 optimal control. The H_2 norm of a system can be interpreted as the rms value of the output when the system is driven by independent zero mean white noise with unit power spectral densities. To associate TMR with the H_2 norm, in the typical HDD shown in Fig. 1, all the NRRO sources are all considered colored noise, which are generated by the white noises passing through their individual filters. Let the disturbance vector be the NRRO sources and the true PES be the output; the transfer function from these noises to the true PES, $y_{\mathrm{PES}\,t}$, is defined as T_{zw}. Thus in the HDD systems, when the number of the collected true PES samples, n in Eq. (2), is large enough, the limit of the H_2 norm of the transfer function T_{zw} is expressed as (Saberi et al., 1995)

$$\|T_{zw}\|_2 = \sqrt{\frac{1}{n-1}\sum_{i=1}^{n} y_{\mathrm{PES}\,t}(i)^2} \tag{2}$$

It is easy to see that the H_2 norm of T_{zw} can be approximated proportional to the standard deviation of the true PES. Therefore, the control design problem to minimize TMR can be treated as an H_2 optimal control problem. Thus, the optimal control problem can be formulated from this illustrated HDD servo system, as shown in Fig. 3 below, and the standard algorithm of H_2 optimal control can be applied.

3. H_2 Output Feedback Optimal Problem and Controller Design

The general H_2 output feedback problem is described as (Saberi et al., 1995)

$$\Sigma : \begin{cases} \dot{x} = Ax + Bu + Ew \\ y = C_1 x + D_1 w \\ z = C_2 x + D_2 u \end{cases} \tag{3}$$

with $x \in \Re^n$ being the state, $u \in \Re^n$ the control input, $\omega \in \Re^l$ the disturbance input, $y \in \Re^p$ the measurement output, and $z \in \Re^q$ the output to be controlled (or controlled output).

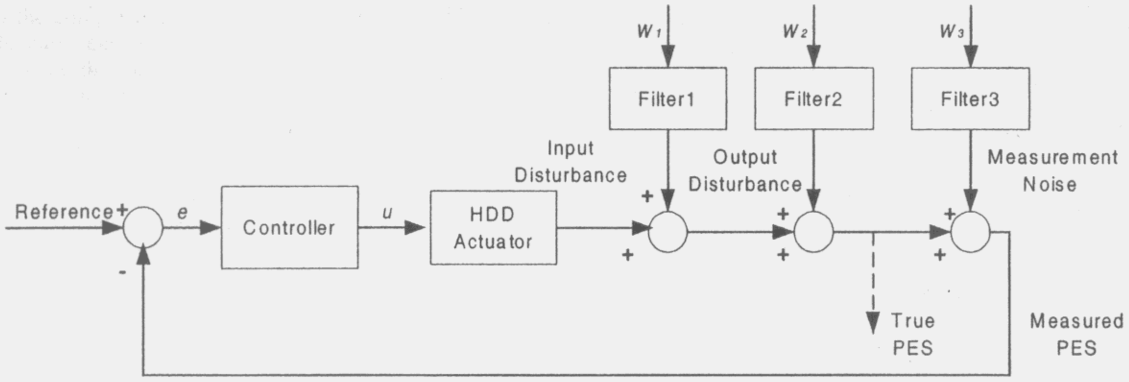

Fig. 2. Simplified disk drive servo system with process disturbance and noise.

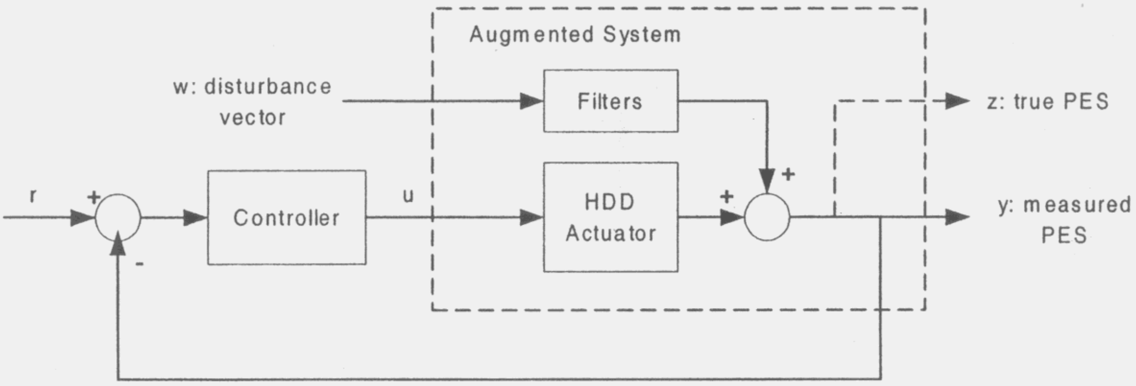

Fig. 3. H_2 output feedback problem of general HDDs.

3.1. Control Design for the Regular Case

According to the developed H_2 optimal control theory, an optimal measurement feedback controller exists in a regular H_2 optimal problem that satisfies the following specific regularity conditions (Saberi et al., 1995).

1. D_2 is injective, that is, D_2 is of maximal column rank.
2. The subsystem (A, B, C_2, D_2) has no invariant zeros on the imaginary axis.
3. D_1 is surjective, that is, D_1 is of maximal row rank.
4. The subsystem (A, E, C_1, D_1) has no invariant zeros on the imaginary axis.

In the case in which the above conditions are not satisfied, the H_2 output feedback problem is called *singular*.

When the problem is regular, the H_2 optimal output feedback controller can be described by

$$\Sigma_c : \begin{cases} \dot{v} = A_c v + B_c y \\ u = C_c v + D_c y \end{cases} \tag{4}$$

with $v \in \Re^k$ being the dynamic order of Σ_c.

By solving the algebra Ricatti equations (AREs) directly (Saberi et al., 1995), we have

$$\Sigma_c : \begin{cases} \dot{v} = (A + BF + KC_1)v - Ky \\ u = Fv \end{cases} \tag{5}$$

where

$$F = -\left(D_2^T D_2\right)^{-1}\left(D_2^T C_2 + B^T P\right) \tag{6}$$

$$K = -\left(QC_1^T + ED_1^T\right)\left(D_1 D_1^T\right)^{-1} \tag{7}$$

and where $P \geq 0$ and $Q \geq 0$ are the solutions of the following AREs, respectively:

$$A^T P + PA - \left(PB + C_2^T D_2\right)\left(D_2^T D_2\right)^{-1} \times \left(D_2^T C_2 + B^T P\right) + C_2^T C_2 = 0 \tag{8}$$

$$QA^T + AQ - \left(QC_1^T + ED_1^T\right)\left(D_1 D_1^T\right)^{-1} \times \left(D_1 E^T + C_1 Q\right) + EE^T = 0 \tag{9}$$

The H_2 norm minimized from the closed-loop transfer matrix $T_{zw}(\Sigma \times \Sigma_c)$ over all stabilizing proper controllers is denoted by γ_2^*:

$$\gamma_2^*: = \inf\{\|T_{zw}(\Sigma \times \Sigma_c)\|_2 \mid \Sigma_c \text{ internally stabilizes } \Sigma\} \tag{10}$$

For the regular problem described above, the minimal H_2 norm, or infimum, of transfer function T_{zw} associated with the output feedback case is given by

$$\|T_{zw}\|_2 = \left\{\text{trace}(E^T P E) + \text{trace}\left[\left(A^T P + PA + C_2^T C_2\right) Q\right]\right\}^{1/2} \tag{11}$$

3.2. Control Design for the Singular Case

When the H_2 optimal problem is singular, the only recourse is to seek a suboptimal controller that guarantees the internal stability of the closed-loop system. Actually, a family of suboptimal controllers can be found that could attain an H_2 norm arbitrarily close to the infimum.

For a sequence of suboptimal controllers to be found, the so-called perturbation method can be applied because of its compactness and elegance. By adding some dummy outputs to z, that is, defining a new control output (Saberi et al., 1995), we have

$$\tilde{z} := \begin{bmatrix} z \\ \epsilon x \\ \epsilon u \end{bmatrix} = \begin{bmatrix} C_2 \\ \epsilon I \\ 0 \end{bmatrix} x + \begin{bmatrix} D_2 \\ 0 \\ \epsilon I \end{bmatrix} u \tag{12}$$

Obviously, if $\epsilon = 0$, we just add some zeros. Sequentially, define another two new matrices:

$$\tilde{E} = [E \quad \epsilon I \quad 0] \quad \text{and} \quad \tilde{D}_1 = [D_1 \quad 0 \quad \epsilon I] \tag{13}$$

Now let us consider the newly constructed perturbed system,

$$\tilde{\Sigma}: \begin{cases} \dot{x} = Ax + Bu + \tilde{E}w \\ y = C_1 x \qquad + \tilde{D}_1 w \\ z = \tilde{C}_2 x + \tilde{D}_2 u \end{cases} \tag{14}$$

where $\tilde{E}$, $\tilde{D}_1$, $\tilde{C}_2$, and $\tilde{D}_2$ are constructed by means of the so-called perturbation approach given before. Obviously, $\tilde{D}_2$ is of maximal column rank and $(A, B, \tilde{C}_2, \tilde{D}_2)$ is free of invariant zeros for any $\epsilon > 0$. Thus, $\tilde{\Sigma}$ satisfies the conditions of the regular output feedback problem, and hence we can apply the previously stated procedures for the regular problem to find appropriate controllers. The controllers works for the original system for sufficiently small ϵ.

3.3. Optimal Control Design Procedure Summary

For the typical HDD system described in the previous section, we can formulate the H_2 problem as follows.

$$\begin{aligned}
x &= (x_{\text{HDD}} \quad x_{\text{ID}} \quad x_{\text{OD}} \quad x_{\text{MN}})' \\
\omega &= (\omega_{\text{ID}} \quad \omega_{\text{OD}} \quad \omega_{\text{MN}})' \\
A &= \begin{pmatrix} A_{\text{HDD}} & \mathbf{0} & \mathbf{0} & \mathbf{0} \\ \mathbf{0} & A_{\text{ID}} & \mathbf{0} & \mathbf{0} \\ \mathbf{0} & \mathbf{0} & A_{\text{OD}} & \mathbf{0} \\ \mathbf{0} & \mathbf{0} & \mathbf{0} & A_{\text{MN}} \end{pmatrix} \\
B &= (B_{\text{HDD}} \quad \mathbf{0} \quad \mathbf{0} \quad \mathbf{0})' \\
E &= \begin{pmatrix} B_{\text{HDD}} & \mathbf{0} & \mathbf{0} \\ B_{\text{ID}} & \mathbf{0} & \mathbf{0} \\ \mathbf{0} & B_{\text{OD}} & \mathbf{0} \\ \mathbf{0} & \mathbf{0} & B_{\text{MN}} \end{pmatrix}' \\
C_1 &= (C_{\text{HDD}} \quad C_{\text{ID}} \quad C_{\text{OD}} \quad C_{\text{MN}}) \\
D_1 &= (D_{\text{ID}} \quad D_{\text{OD}} \quad D_{\text{MN}}) \\
C_2 &= (C_{\text{HDD}} \quad C_{\text{ID}} \quad C_{\text{OD}} \quad \mathbf{0}) \\
D_2 &= \mathbf{0}
\end{aligned} \tag{15}$$

Here the state vector x, $\{x_{\text{HDD}}, x_{\text{ID}}, x_{\text{OD}}, x_{\text{MN}}\}'$, are the state variables from the actuator, input disturbance filter, output disturbance filter, and measurement filter in Fig. 2. The disturbance vector ω, $\{\omega_{\text{ID}}, \omega_{\text{OD}}, \omega_{\text{MN}}\}'$, includes the white noise sources that take effect before the process disturbance filter and the measurement noise filter. Here $\Sigma_{\text{HDD}}(A_{\text{HDD}}, B_{\text{HDD}}, C_{\text{HDD}}, D_{\text{HDD}})$, $\Sigma_{\text{ID}}(A_{\text{ID}}, B_{\text{ID}}, C_{\text{ID}}, D_{\text{ID}})$, $\Sigma_{\text{OD}}(A_{\text{OD}}, B_{\text{OD}}, C_{\text{OD}}, D_{\text{OD}})$, and $\Sigma_{\text{MN}}(A_{\text{MN}}, B_{\text{MN}}, C_{\text{MN}}, D_{\text{MN}})$ denote the disk drive actuator, the input disturbance filter, the output disturbance filter, and the measurement noise filter individually, and all these plants are assumed strictly proper. In the problem formulation, the input disturbance is considered as a lumped disturbance on the plant output.

In many cases, because of the high gain property of the voice coil motor (VCM) plant, the optimal solution cannot easily be obtained by solving the AREs. It is quite common to find a suboptimal output feedback controller for a given HDD plant. For the ease of application, the optimal control design procedure of both the regular and singular systems can be summarized as follows.

- Step 1: Establish the actuator model, disturbance model, and measurement noise model.
- Step 2: Formulate the standard H_2 optimal problem, as described by Eq. (15).
- Step 3: Check the regularity property of the resulting H_2 optimal problem.
- Step 4: If the H_2 optimal problem is regular, the resultant output feedback controller is given in Eq. (5) by

solving the related Riccati equations, Eqs. (8) and (9). Otherwise, for a singular H_2 problem, augment the plant output to make the problem regular. Solve the Riccati equations (8) and (9) to find an H_2 suboptimal controller. Reduce ϵ by half and solve Eqs. (8) and (9) each time, until the resulting H_2 norm of the resultant controller converges within the calculation precision.

Step 5: If the problem is ill conditioned, use the time-scaling (substitute t with $\tau = \omega_0 t$ in a Laplace transformation; see Franklin et al., 1994, p. 67) method to reduce the ill numerical condition until these Ricatti equations can be solved.

After the optimal or suboptimal controller is obtained, time-domain and frequency-domain simulations can be performed to check the performance of the controller before implementation.

4. Application Examples

In this section, we use the proposed algorithm to design the output feedback controllers for two types of typical HDD systems, one with a single- stage actuator and the other with a dual-stage actuator. With all the disturbance and measurement noise filters included in the optimal problem, both the single-stage H_2 problem and dual-stage H_2 problem were singular. Thus we can only find suboptimal output feedback controllers. By tuning the parameter ϵ in Eqs. (12) and (13) smaller, we find that the resulting TMR decreases and approaches the minimum.

4.1. Single-Stage Actuator Case

First, we formulate the H_2 problem in the single-stage actuator system. In such a system, the VCM works as the only actuator to drive the head assembly and the slider. The structure of such a servo system is similar to the system shown in Fig. 2, with the VCM as the HDD actuator.

The transfer function of the VCM (see Fig. 4) is as follows:

$$G_{\mathrm{VCM}}(s) = \frac{2.834 \times 10^{-5}s^6 + 0.8529s^5 - 3.742 \times 10^4 s^4 + 2.423 \times 10^9 s^3 - 0.627 \times 10^{14} s^2 + 6.662 \times 10^{17} s + 2.851 \times 10^{24}}{s^6 + 1.011 \times 10^4 s^5 + 4.214 \times 10^9 s^4 + 3.35 \times 10^{13} s^3 + 1.807 \times 10^{18} s^2 + 9.128 \times 10^{19} s + 2.851 \times 10^{22}} \quad (16)$$

In the optimal control design described in this paper, the filter models of the input disturbance, output disturbance, and measurement noise will play the vital roles. Here the approximate filter models of the NRRO sources

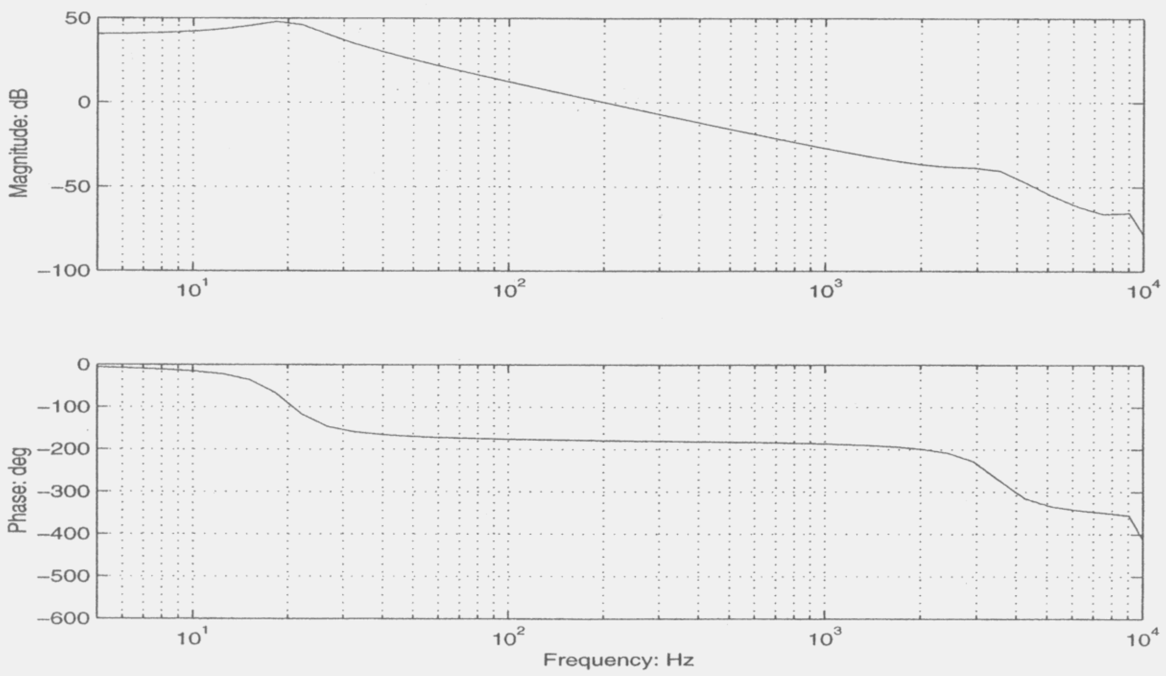

Fig. 4. Bode plot of the VCM.

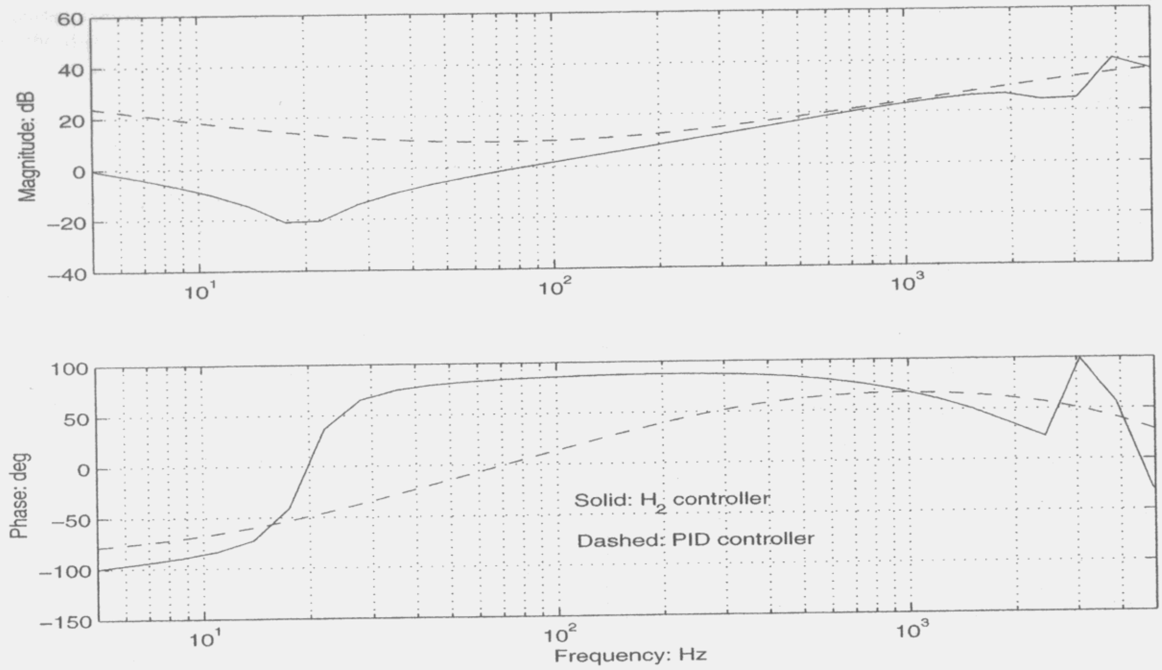

Fig. 5. H_2 and PID controllers in the single-stage case.

are obtained from the measured PES data in a commercial HDD. They are denoted as $G_{ID}(s)$, $G_{OD}(s)$, and $G_{MN}(s)$ individually, as shown in Eq. (19).

$$G_{ID}(S) = \frac{72400s^2 + 4.4 \times 10^8 s - 1.21 \times 10^{13}}{s^3 + 59000s^2 + 8 \times 10^8 s + 4.13 \times 10^9} \tag{17}$$

$$G_{OD}(s) = \frac{62500s^2 - 1.28 \times 10^9 s + 1.92 \times 10^{13}}{s^3 + 35400s^2 + 1.68 \times 10^9 s + 3.85 \times 10^{12}} \tag{18}$$

$$G_{MN}(s) = \frac{9280s^2 - 4.08 \times 10^8 s + 6.89 \times 10^{12}}{s^3 + 6210s^2 + 4.06 \times 10^8 s + 1.21 \times 10^{12}} \tag{19}$$

Then the proposed optimal control design in the previous section is applied. During the control design, to approach the limit of the suboptimal controller, we push the ϵ until there is no solution to the Riccati equations (8) and (9). Finally, the ϵ at 5×10^{-8} returns a suboptimal H_2 output feedback controller that is considered nearly optimal, as shown in Fig. 5.

The bode plots of the open-loop compensated system, and the sensitivity and complementary sensitivity functions, are shown in Fig. 6 and Fig. 7, respectively. The phase margin and gain margin of the open-loop compensated system by this H_2 controller are 75° and 15 dB, respectively. In Fig. 7, the difference of the slopes of the sensitivity functions of H_2 and proportional, integral, and differential (PID) control in the low frequency is due to the different design methods. During the proposed H_2 optimal design, in order to obtain the minimized TMR, we added no integrator to improve the system performance in the low frequency. We then discretized it by using bilinear transformation with the sampling frequency at 15 kHz.

A PID controller is used for comparison here. This PID controller has a usual structure and was tuned to have a fast time response and small overshoot. It is given by

$$G_{PID}(z) = \frac{1.667 \times 10^{-5} z^2 - 3.202 \times 10^{-5} z + 1.536 \times 10^{-5}}{4.211 \times 10^{-7} z^2 - 4.211 \times 10^{-7} z} \tag{20}$$

with its bode plot shown in Fig. 5.

As a way to show the performance of H_2 controller tracking, the time responses of a step reference of both the H_2 controller and PID controller are shown in Fig 8. The spectra and histogram of the true PES by the H_2 controller is shown in Figs. 9 and 10.

To show that the obtained controller is close to the "optimal" one, we let the parameters in the estimator and the controller randomly vary within ±10% and ±5%; the resulting $3\sigma_{PEST}$, is shown in Fig. 11. Thus we found that the obtained H_2 output feedback controller can give us

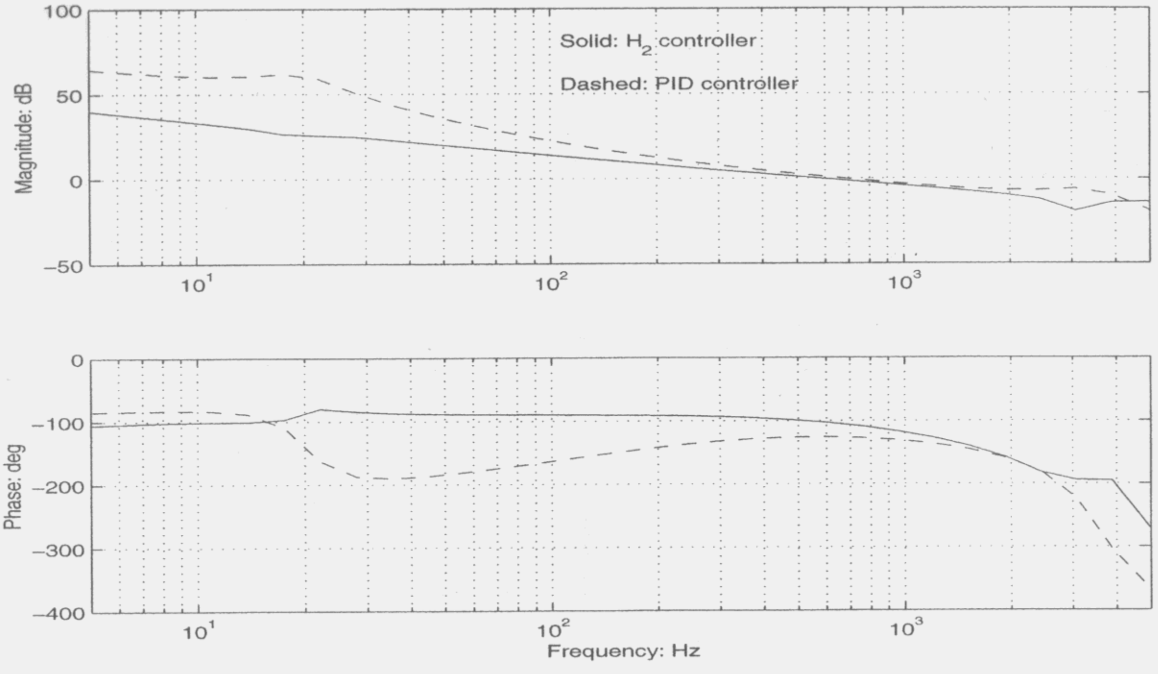

Fig. 6. Bode plot of compensated open-loop systems by H_2 and PID control in the single-stage case.

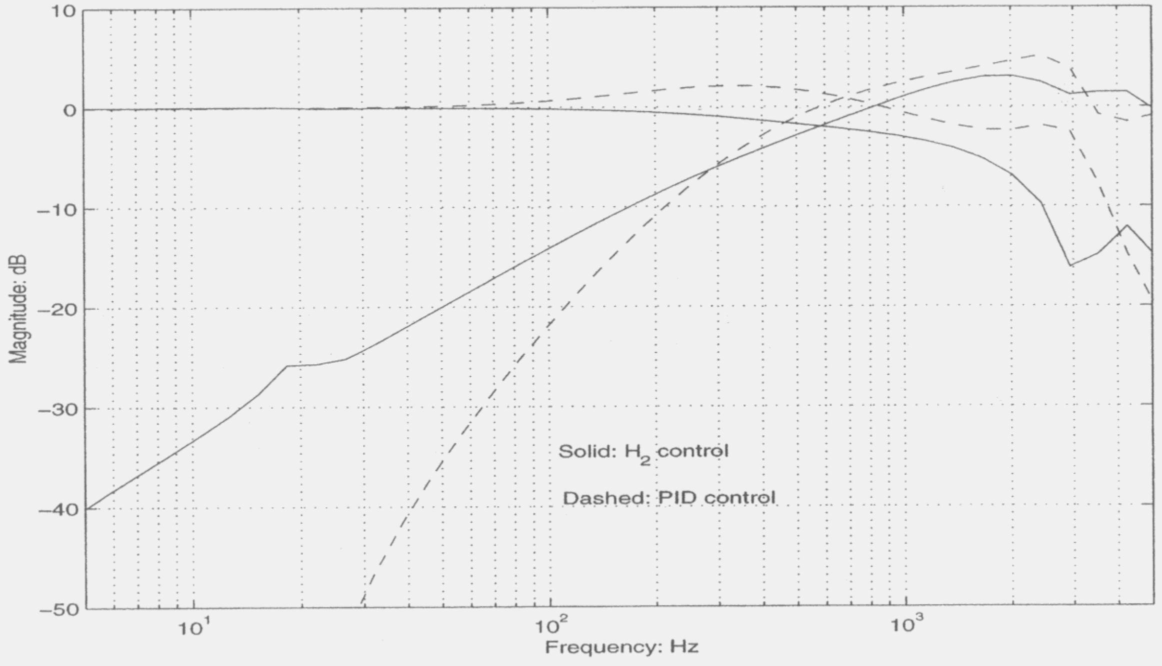

Fig. 7. Functions of sensitivity and complementary sensitivity by H_2 and PID control in the single-stage case.

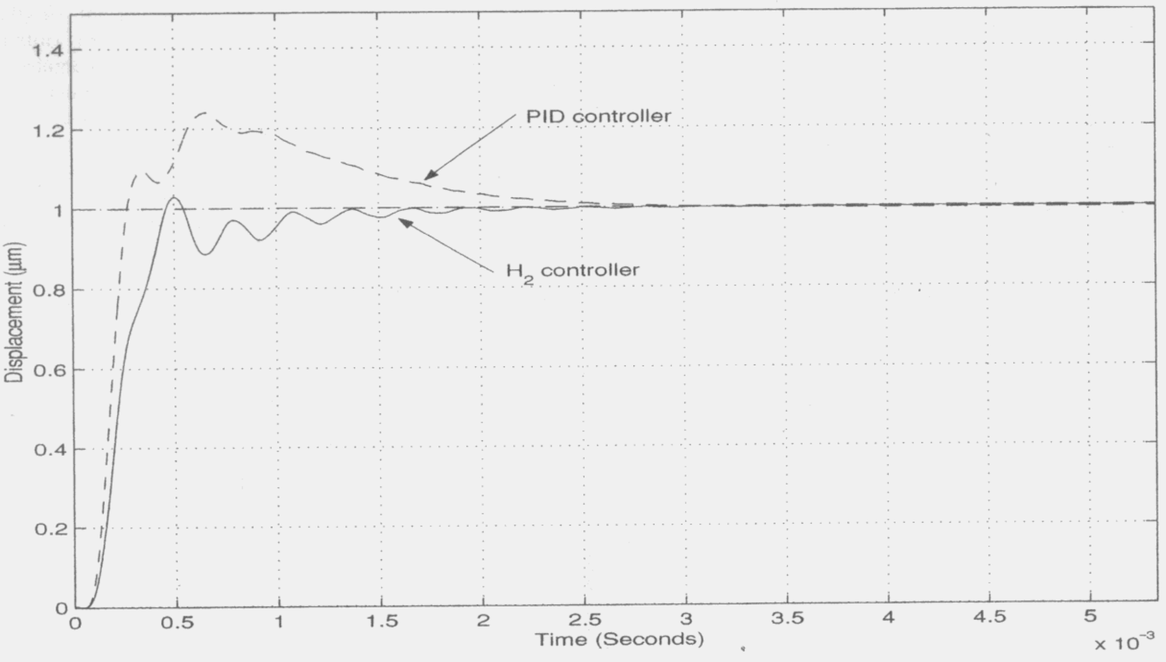

Fig. 8. Step responses of a compensated system by H_2 and PID control.

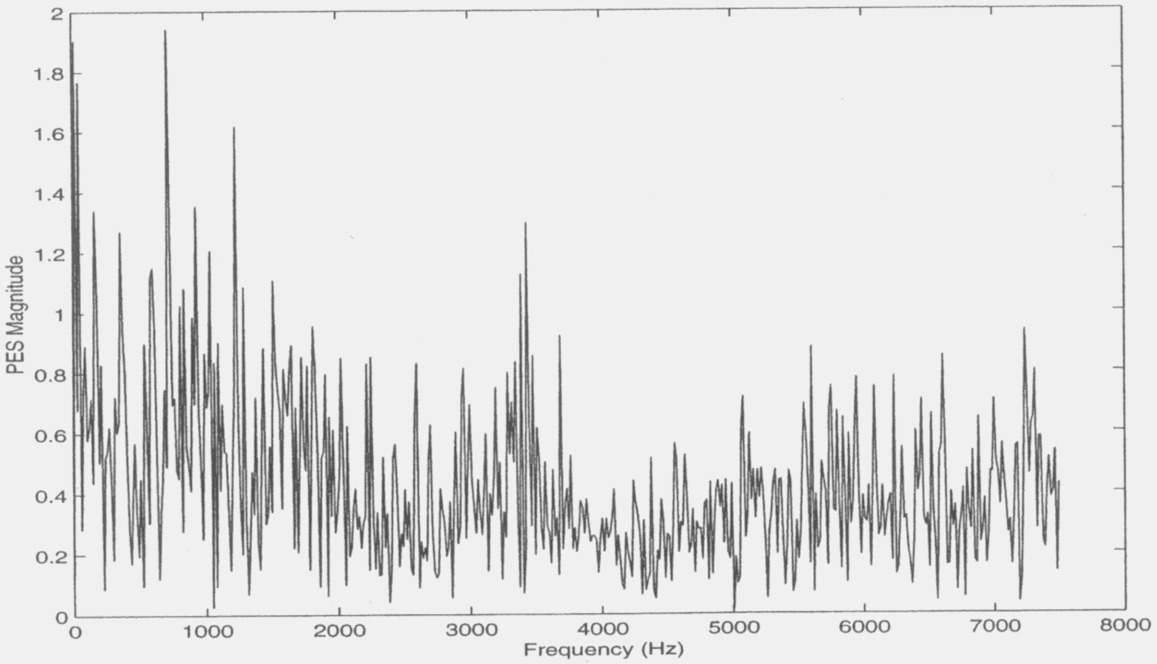

Fig. 9. Spectrum of the true PES by H_2 control in the single-stage case.

the minimal TMR. This verifies the described theory that we can obtain a nearly optimal controller by pushing the tuning parameter ϵ smaller; thus the obtained H_2 norm approaches the optimal value in a certain range.

4.2. Dual-Stage Actuator Case

Consider the dual-stage actuator system as shown in Fig. 12. In the dual-stage actuator, a piezoelectric micro

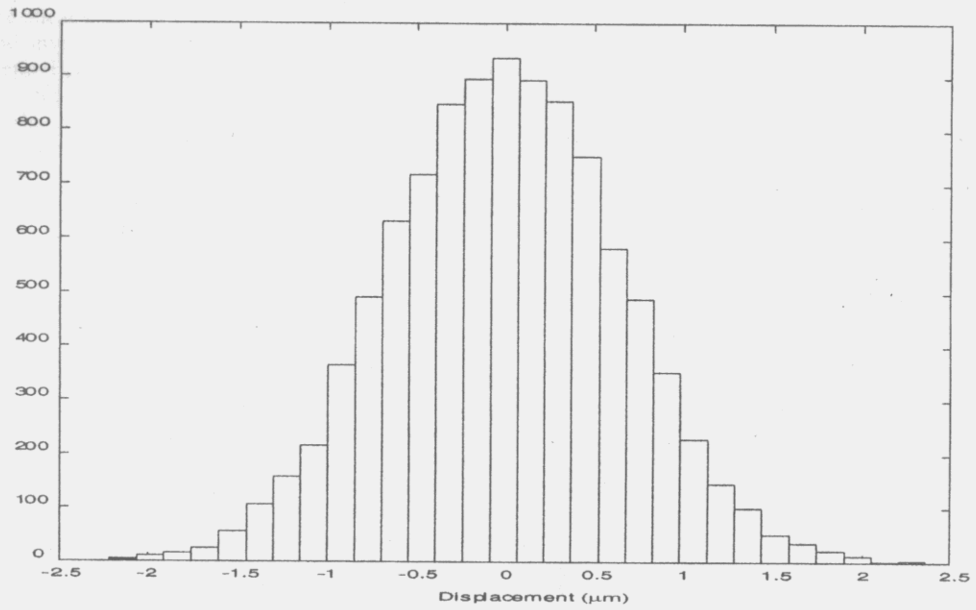

Fig. 10. Histogram of the true PES by H_2 control in the single-stage case.

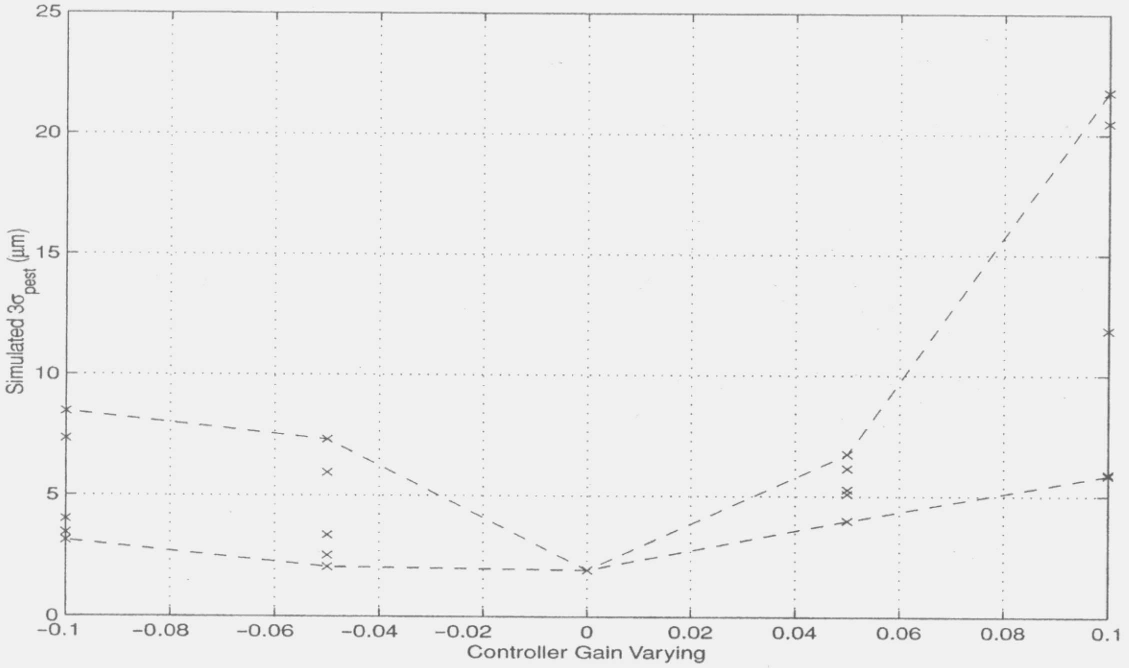

Fig. 11. Simulated TMR against the controller parameters' variation.

actuator (MA) works in tandem with the VCM to do the fine positioning, while VCM does the coarse positioning (Aggarwal et al., 1997; Evans et al., 1999; Hernandez et al., 1999; Horsley et al., 1999; Semba et al., 1999).

Here the whole dual-stage actuator is considered as a dual input, single output (DISO) system, where the two inputs, u_{VCM} and u_{MA}, are the control signals to control the VCM and the MA individually. Thus by following the guideline as in Eq. (15), we can formulate

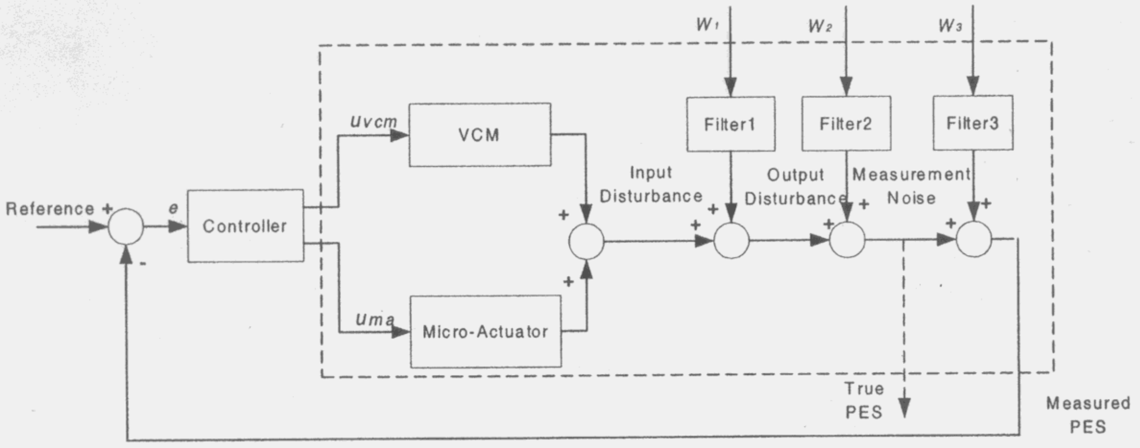

Fig. 12. H_2 output feedback problem of a dual-stage actuator.

the H_2 problem in the dual-stage actuator. We use $\Sigma_{MA}(A_{MA}, B_{MA}, C_{MA}, D_{MA})$ to denote the MA; the dual-stage actuator, denoted by Σ_{HDD}, is described by

$$A_{HDD} = \begin{pmatrix} A_{VCM} & \mathbf{0} \\ \mathbf{0} & A_{MA} \end{pmatrix}$$
$$B_{HDD} = \begin{pmatrix} B_{VCM} & \mathbf{0} \\ \mathbf{0} & B'_{MA} \end{pmatrix}$$
$$C_{HDD} = (C_{VCM} \quad C_{MA})$$
$$D_{HDD} = (0 \quad 0) \tag{21}$$

For the dual-stage actuator system in the example, all the models of the VCM, noise filter, and disturbance filter are the same. The model of the MA $G_{MA}(s)$ in Eq. (22) is a fourth-order one, as shown in Fig. 13.

and MA into consideration during the design. Thus, to find a more practical control for the implementation purpose, we consider the H_2 optimal control by using the PQ method (Schroeck and Messner, 1999) in the following section.

4.3. Dual-Stage Case: H_2 Design by Using the PQ Method

To make the H_2 optimal design work more implementable in the dual-stage case, H_2 control by using the PQ method is proposed. As shown in Fig. 16, the first step of the control design is to simultaneously choose the C_1 and C_2 to address the relative output contribution of the VCM and MA. Then, we apply the proposed H_2 optimal design

$$G_{MA}(s) = \frac{-0.3352s^4 + 16400s^3 + 1.052 \times 10^9 s^2 + 3.376 \times 10^{13} s + 3.472 \times 10^{18}}{s^4 + 2460s^3 + 2.99 \times 10^9 s^2 + 4.14 \times 10^{12} s + 1.81 \times 10^{18}} \tag{22}$$

Because of the high order of the H_2 problem in the dual-stage actuator, we push the ϵ until 1×10^{-3} before there is no solution to the Ricatti equations. The obtained H_2 output feedback controllers for the VCM and MA are shown in Fig. 14, together with the open-loop compensated system.

The phase margin (95°) and gain margin (22 dB) are even better than the single-stage system, showing a better robustness performance. The histogram of the true PES is shown in Fig. 15. It is found that during the track-following mode, the MA does most of the positioning work while the VCM actuator works less (Fig. 19). Compared with the published control design work on the dual-stage actuator, the control design results appear different because we have not taken any weighting functions of the VCM

to find a controller for the equivalent single input, single output (SISO) system shown in Fig. 16.

Following the PQ method, we choose the transfer function of $C_1(s)$ as

$$C_1(s) = \frac{105.4s^2 + 1.211 \times 10^5 s + 5.206 \times 10^7}{s^2 + 7613s + 1.449 \times 10^7}, \tag{23}$$

and we choose $C_2(s)$ as 1.

Then, the parallel structures of the VCM with $C_1(s)$ and the MA with $C_2(s)$ are equivalent to a SISO system. The proposed H_2 control illustrated in the single-stage case is applied and the controller is found. The step response of the compensated dual-stage actuator system is shown in

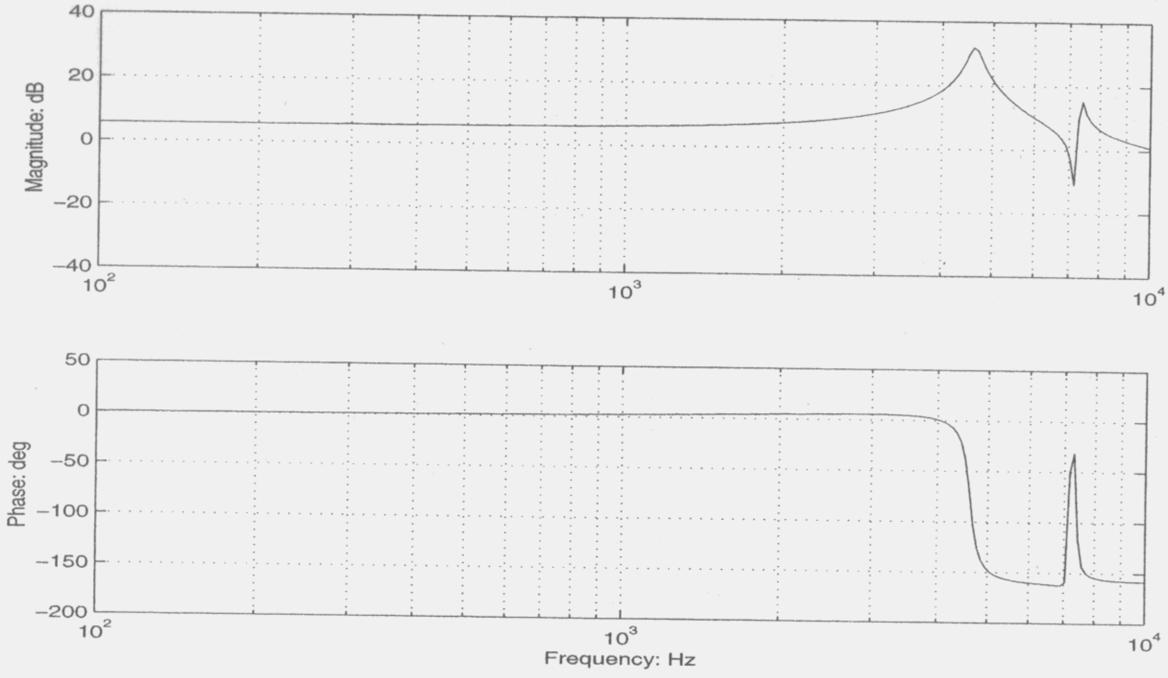

Fig. 13. Bode plot of the MA.

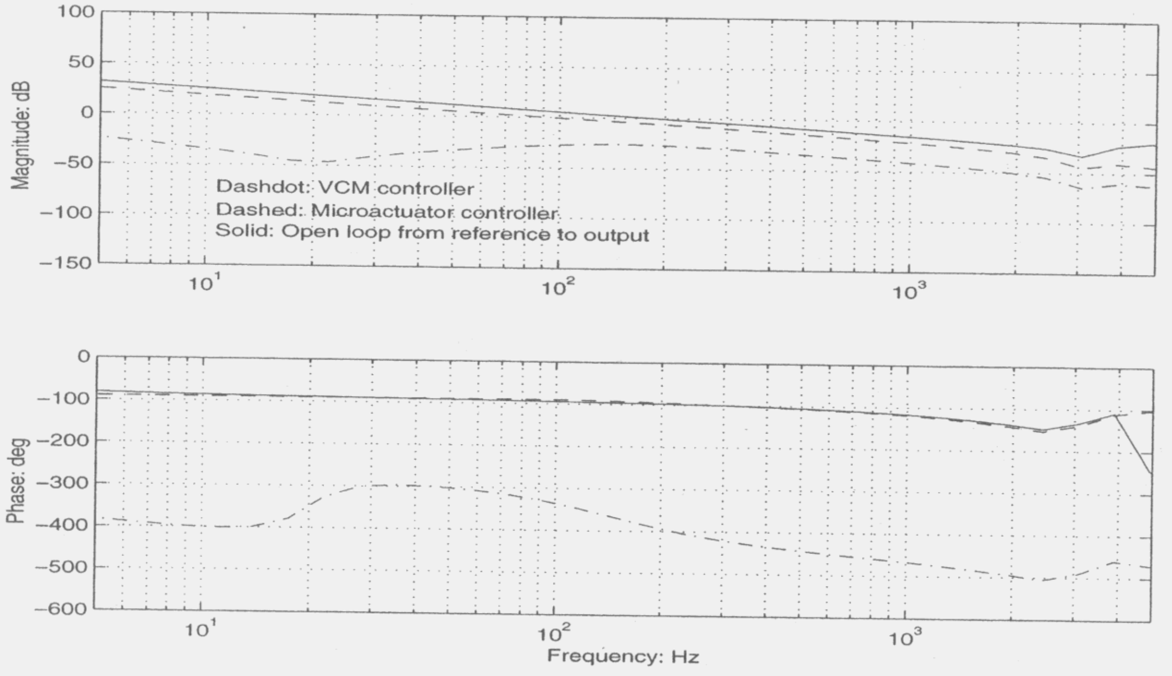

Fig. 14. Bode plots of the VCM controller, MA controller, and open-loop compensated system.

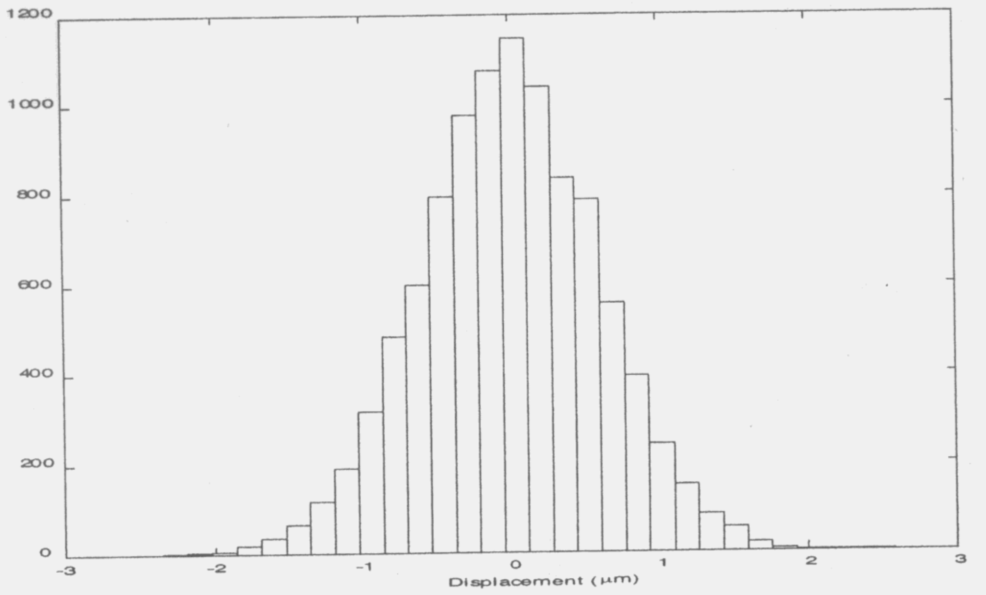

Fig. 15. Histogram of the true PES by H_2 in a dual-stage actuator.

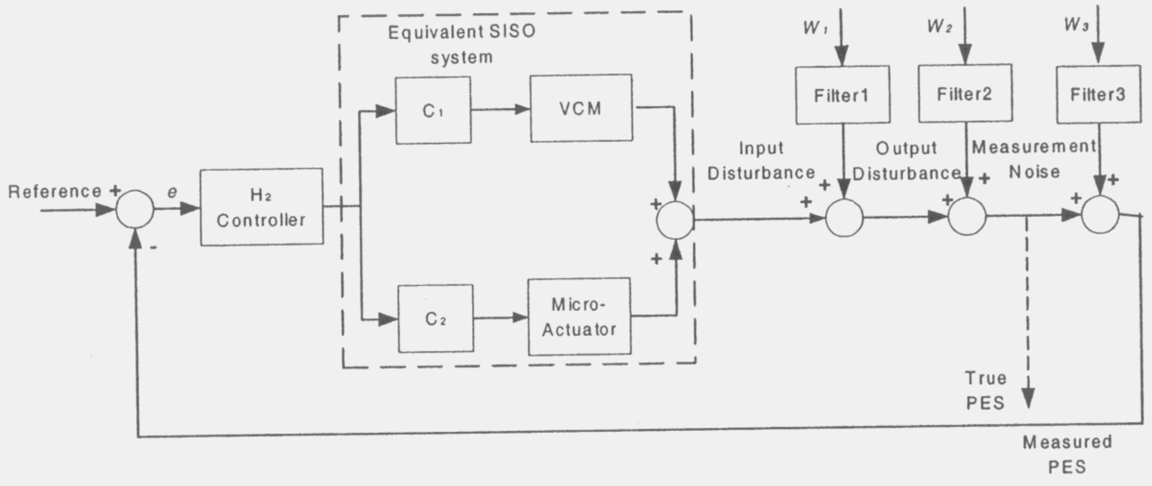

Fig. 16. H_2 and PQ method compensated system block diagram.

Fig. 17. The bode plots of the controllers for the VCM and the MA, together with the open-loop compensated system, are shown in Fig. 18.

The summary of the controllers' performance is shown in Table 1 (where 1 μin. = 25.4 nm). The theoretical TMRs in the second column of Table 1 are calculated from the obtained H_2 norms by use of Eq. (11). From Table 1, it is found that compared with PID control, the proposed H_2 optimal control design could improve the TMR budget by ~10% in the single-stage case. Furthermore, it is found that the dual-stage actuator HDD can achieve a higher TPI rate than that of the single-stage actuator. Because the suboptimal controller in the dual-stage case has not been tuned optimally enough as a result of the ill condition, the compensated dual-stage actuator system has only approximately <10% improvement in TMR than the single-stage case. Last, the resulting TMR of the H_2 control by using

Table 1. Summary of controller performances

Parameter	Measured TMR (μin.)	Theoretical TMR (μin.)
PID (single stage)	2.11	—
H_2 control (single stage)	1.93	1.81
H_2 control (dual stage)	1.79	1.73
H_2, using PQ (dual stage)	1.98	1.96

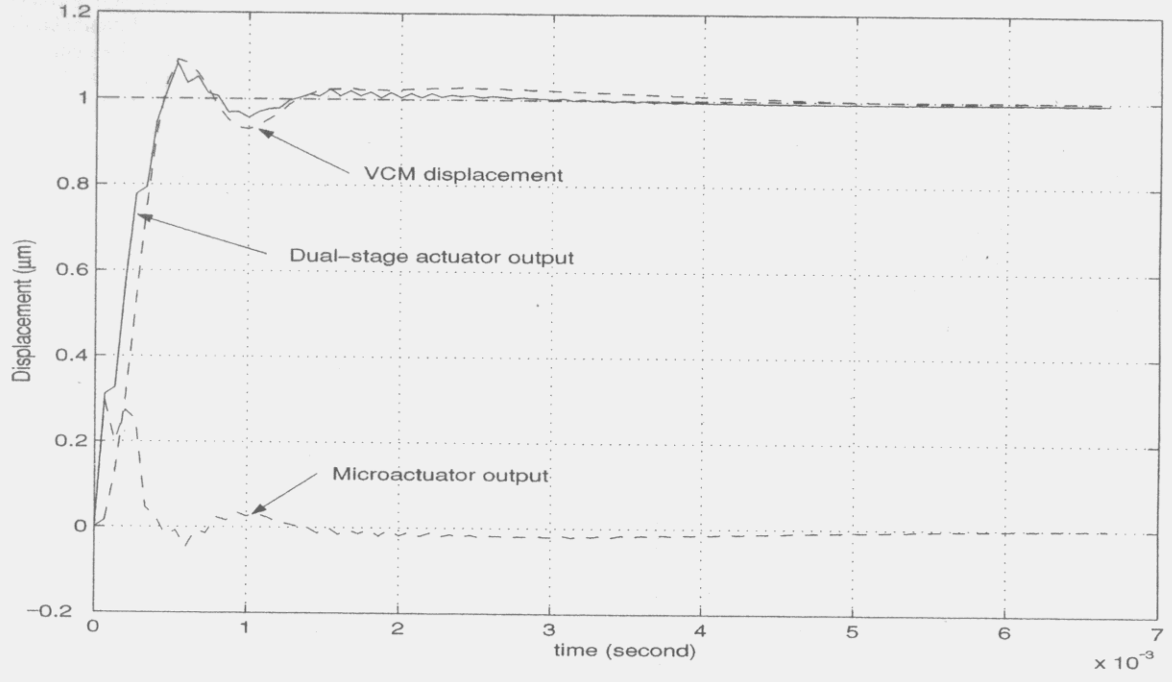

Fig. 17. Step responses of H_2, using the PQ method compensated system.

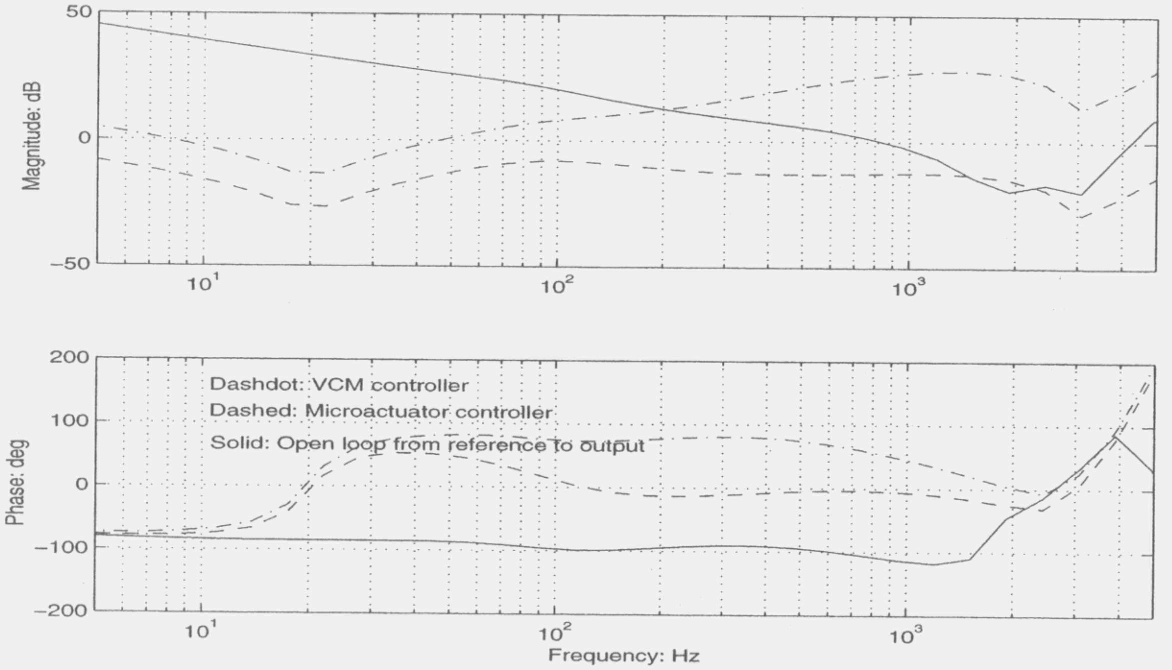

Fig. 18. Bode plots of controllers and open-loop transfer functions by H_2, using the PQ method.

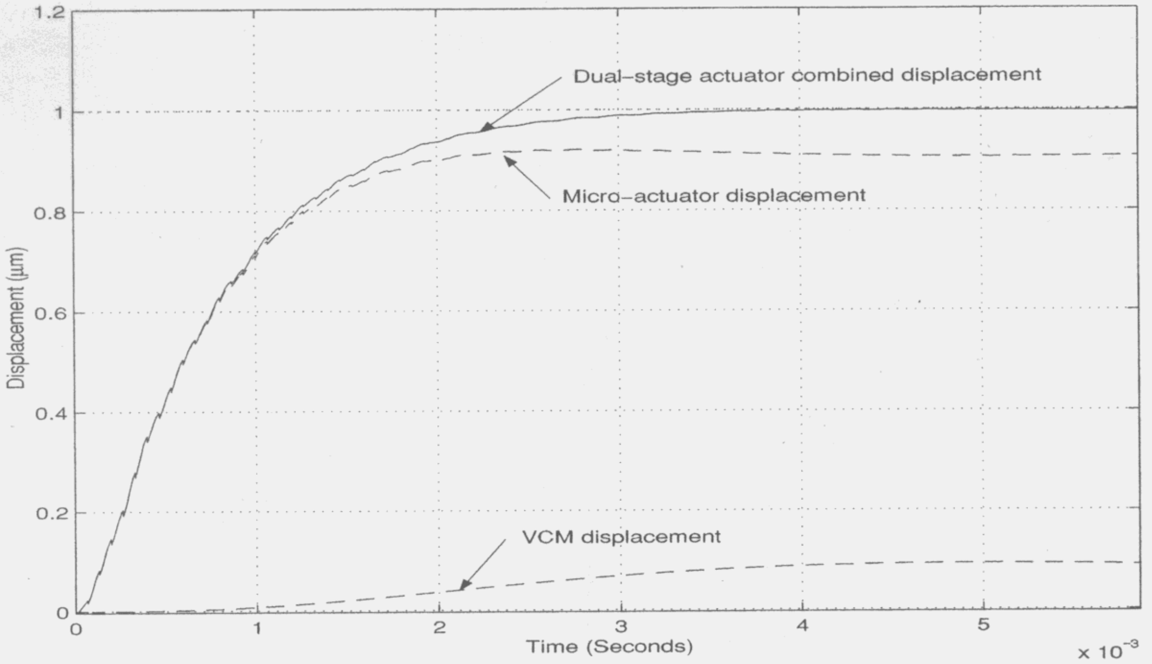

Fig. 19. Step response of the H_2 compensated system in the dual-stage case.

the PQ method is shown. In the system compensated by H_2 control with the PQ method, we cannot establish the direct relationship between the H_2 norm and TMR budget. Thus it is not surprising that the TMR improvement by H_2 by using the PQ method is even less than that in the single-stage case.

5. Summary and Discussion

In this paper we consider the problem of finding the highest achievable TPI rate or equivalently the lowest TMR rate, by means of H_2 optimal control. We showed that finding the highest achievable TPI rate can be formulated and solved as an H_2 optimal control problem when we consider the track-following problem caused by HDD internal disturbance and noise sources. For our case, the optimal control problem is singular and thus a family of suboptimal H_2 controllers can be found. By proper tuning, the resulting H_2 norms are very close to the minimum.

Two application examples, of both the single-stage case and the dual-stage case, are given to find the limit of the TPI rate, although the resultant controller may not be practical because the design procedure did not consider factors other than track-following accuracy. The proposed algorithm can be used to find a benchmark for the evaluation of other linear design work toward higher TPI rates in the HDD servo.

References

Abramovitch, D., Hurst, T., and Henze, D. (1997), "Decomposition of Baseline Noise Sources in Hard Disk Position Error Signals using the PES Pareto Method," *Proc. American Control Conf.* **5**, 2901–2905.

Aggarwal, S.K., Horsley, D.A., Horowitz, R., and Pisano, A.P. (1997), "Micro-Actuators for High Density Disk Drives," *Proc. American Control Conf.* **5**, 3979–3984.

Chang, J-K., Weerasooriya, S., and Ho, H.T. (1997), "Improved TMR Budget Through a Frequency Shaped Servo Design," *Proc. 23rd IEEE Conf. IECON* **1**, 47–51.

Chang, J-K. and Ho, H.T. (1999), "LQG/LTR Frequency Loop Shaping to Improve TMR Budget," *IEEE Trans. Magn.* **35**, 2280–2282.

Chen, R., Guo, G., and Low, T.S. (1999), "Intersample Ripple Free Multirate Control for HDD Servo System," *Proc. 25th IEEE Conf. IECON* **3**, 1171–1176.

Ehrlich, R. and Curran, D. (1999), "Major HDD Sources and Projected Scaling with TPI," *IEEE Trans. Magn.* **35**, 885–891.

Evans, R.B., Griesbach, J.S., and Messner, W.C. (1999), "Piezoelectric Microactuator for Dual-Stage Control," *IEEE Trans. Magn.* **35**, 977–982.

Franklin, G.F., Powell, J.D., and Emami-Naeini, A. (1994), *IEEE Feedback Control of Dynamic Systems*, Addison-Wesley, Reading: MA.

Fujimoto, H., Hori, Y., Yamaguchi, T. and Nakagawa, S. (1999), "Proposal of Perfect Tracking and Perfect Disturbance Rejection Control by Multirate Sampling and Applications to Hard Disk

Drive Control," *Proc. 38th IEEE Conf. Decision Control* **5**, 5277–5282.

Goh, T.B., Li, Z.M., Chen, B.M., Lee, T.H., and Huang, T. (1999), "Design and Implementation of a Hard Disk Drive Servo System Using Robust and Perfect Tracking Approach," *Proc. 38th IEEE Conf. Decision Control* **5**, 5247–5252.

Guo, L. (1997), "A New Disturbance Rejection Scheme for Hard Disk Drive Control," *IEEE Trans. Mechatron.* **2**, 77–85.

Guo, L., Lee, S.H., Hudson, A., and Chen, S.H. (1999), "A Comprehensive Time-Domain Simulation Tool for HDD Servo Control Design and Mechanical Enhancement," *IEEE Trans. Magn.* **35**, 879–884.

Hara, T. and Tomizuka, M. (1999), "On the Performance Enhancement of Multi-Rate Controller for Hard Disk Drives," *IEEE Trans. Magn.* **35**, 898–903.

Ho, H.T. (1997), "Noise Impact on Servo TMR," *Proc. American Control Conf.* **5**, 2906–2909.

Hernandez, D., Park, S.S., Horowitz, R., and Packard, A.K. (1999),"Dual-Stage Track-Following Servo Design for Hard Disk Drives," *Proc. American Control Conf.* **6**, 4116–4121.

Horsley, D.A., Hernandez, D., Horowitz, R., Packard, A.K., and Pisano, A.P. (1999), "Closed-Loop Control of a Microfabricated Actuator for Dual-Stage Hard Disk Drive Servo Systems," *Proc. American Control Conf.* **5**, 3028–3032.

Hurst, T., Abramovitch, D., and Henze, D. (1997), "Measurements for the PES Pareto Method of Identifying Contributors to Disk Drive Servo System Errors," *Proc. American Control Conf.* **5**, 2896–2900.

Iwashiro, M., Yatsu, M., and Suzuki, H. (1999), "Time Optimal Track-to-Track Seek Control by Model Following Dead-Beat Control," *IEEE Trans. Magn.* **35**, 904–909.

Lin, C., Guo, G., Chen, B.M., and Ko, C.C. (2000), "Optimal Track Following Control for Hard Disk Drives," *Proc. 6th Int. Workshop on Advanced Motion Control (AMC'00)*, pp. 502–506, Nagoya, Japan.

McAllister, J.S. (1997), "Disk Flutter: Causes and Potential Cures," *Data Storage*, **May/June**, 29–34.

McAllister, J.S. (1996), "The Effects of Disk Platter Resonances on Track Misregistration in 3.5 Inch Disk Drives," *IEEE Trans. Magn.* **32**, 1762–1766.

Saberi, A., Sannuti, P., and Chen, B.M. (1995), *H_2 Optimal Control*, Prentice-Hall, Englewood Cliffs, NJ.

Semba, T., Hirano, T., Hong, J., and Fan, L-S. (1999), "Dual-Stage Servo Controller for HDD Using MEMS Microactuator," *IEEE Trans. Magn.* **35**, 2271–2273.

Schroeck, S.J. and Messner, W.C. (1999),"On Controller Design for Linear Time-Invariant Dual-Input Single-Output Systems," *Proc. American Control Conf.* **6**, 4122–4126.

Yamaguchi, T., Tomiyama, F., Numasato, H., Hamada, Y., Shishida, K., Usui, K., and Hirai, H. (1999), "Modeling and TMR Budget Design for Head Positioning of High Track-Density Disk Drives," *IEEE Trans. Magn.* **35**, 892–897.